Supplementary Figure 1

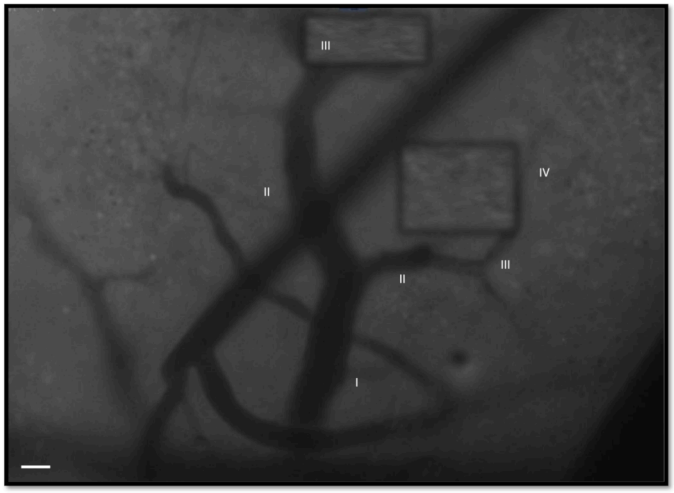

Fig. S1. HEV trees of the inguinal lymph node

Identification of the HEV with different diameters (from the narrow IV to wide I) in the inguinal lymph nodes of the WT host mice (Objective 40X). Scale bar: 25 μm.

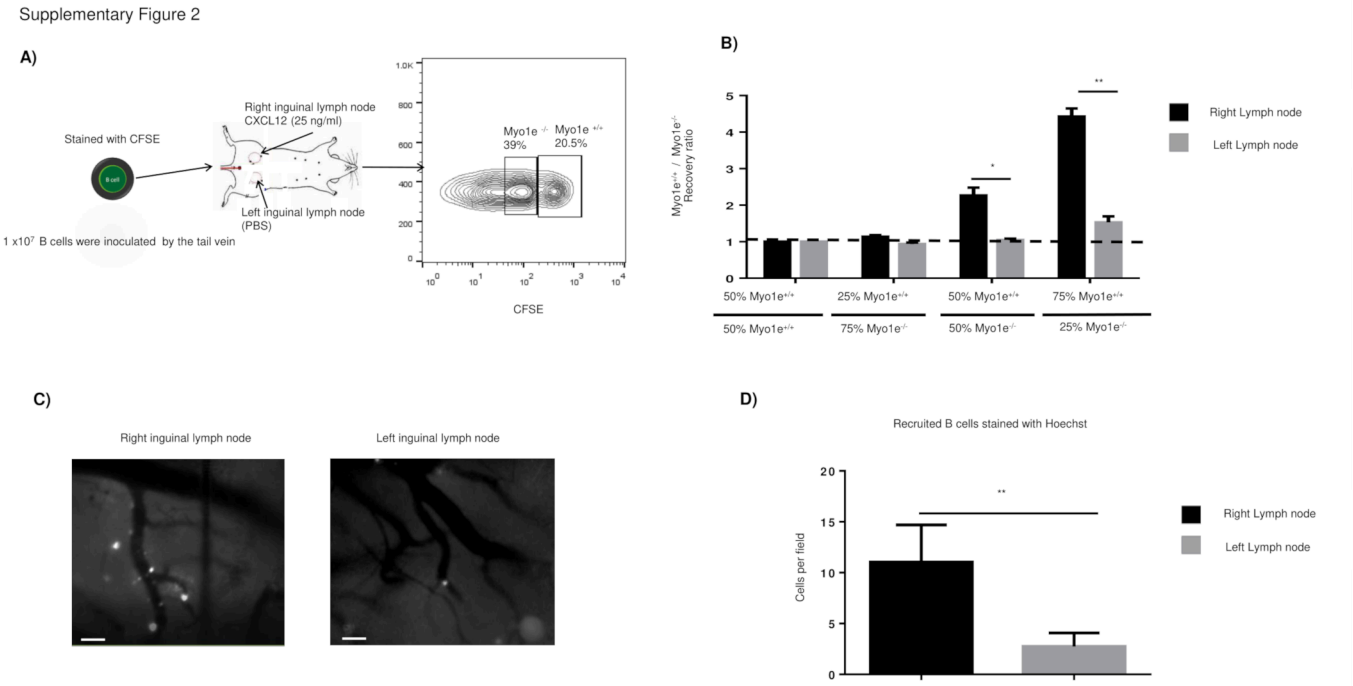

Fig. S2. Myo1e participates in the recruitment of B cells to the inguinal lymph node in response to CXCL12

A) Schematic representation of the injection of activated and CFSE-stained B cells from of Myo1e$^{+/+}$ and Myo1e$^{-/-}$ mice. B) Adoptive transfer of activated B cells from Myo1e$^{+/+}$ and Myo1e$^{-/-}$ mice at different proportions (25%, 50%, and 75%) into the host mice; B cells were previously labeled with different concentrations of CFSE (0.6 µM for Myo1e$^{+/+}$ and 0.1 µM for Myo1e$^{-/-}$ or *vice versa*). One hour before B cell injection, the right inguinal lymph node was injected with CXCL12 and the left inguinal lymph node with PBS. Two hours later, the cells were recovered from each inguinal lymph node, and labeled B cells were identified and measured in each organ by flow cytometry. The recovery ratio was calculated by dividing the absolute numbers of Myo1e$^{+/+}$ to the absolute numbers of Myo1e$^{-/-}$ B cells; n=5. Data are mean ± SD. **p<0.01 *p<0.05. C). Representative images of activated B cells from Myo1e$^{+/+}$ and Myo1e$^{-/-}$ mice stained with CFSE and recruited to the right and left inguinal lymph node of the host mouse. (40x objective). Scale bars: 25 µm, n=5. D) Total of activated B cell (Hoechst33342-labeled) recruited to the right or left inguinal lymph node (independently if they were from Myo1e$^{+/+}$ or Myo1e$^{-/-}$). The data are representative of 12 fields for each experiment; n=5. Data are mean ± SD **p<0.01.

Supplementary Figure 3

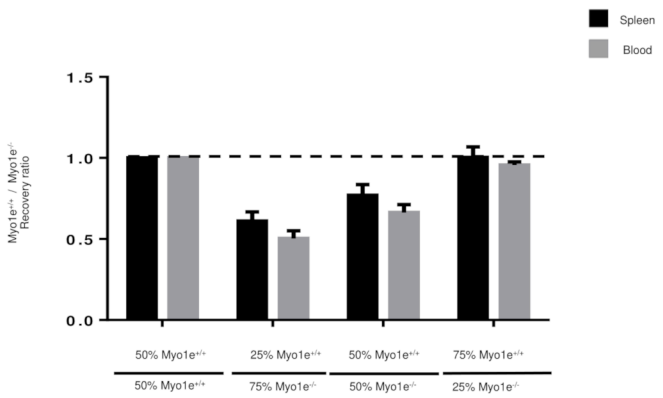

Fig. S3. Number of circulating B cells from Myo1e$^{+/+}$ and Myo1e$^{-/-}$ mice in the spleen and the blood

Adoptive transfer of activated B cells from Myo1e$^{+/+}$ and Myo1e$^{-/-}$ mice at different proportions (25%, 50%, and 75%) in the host mice. B cells were previously labeled with varying concentrations of CFSE (0.6 µM Myo1e$^{+/+}$ and 0.1 µM Myo1e$^{-/-}$ and vice versa). One hour before B cell injection, the right inguinal lymph node was inoculated with CXCL12 and the left inguinal lymph node with PBS. After 2 hours, the cells were recovered from the spleen and the blood and quantified. B cells were identified based on the CFSE-staining level, and the recovery ratio of each organ was measured by flow cytometry. The recovery ratio for each mix is shown in the graphics. The recovery ratio was calculated, dividing the absolute numbers of Myo1e$^{+/+}$ between the total numbers of Myo1e$^{-/-}$ B cells; n=5. Data are mean ± SD.

Supplementary Figure 4

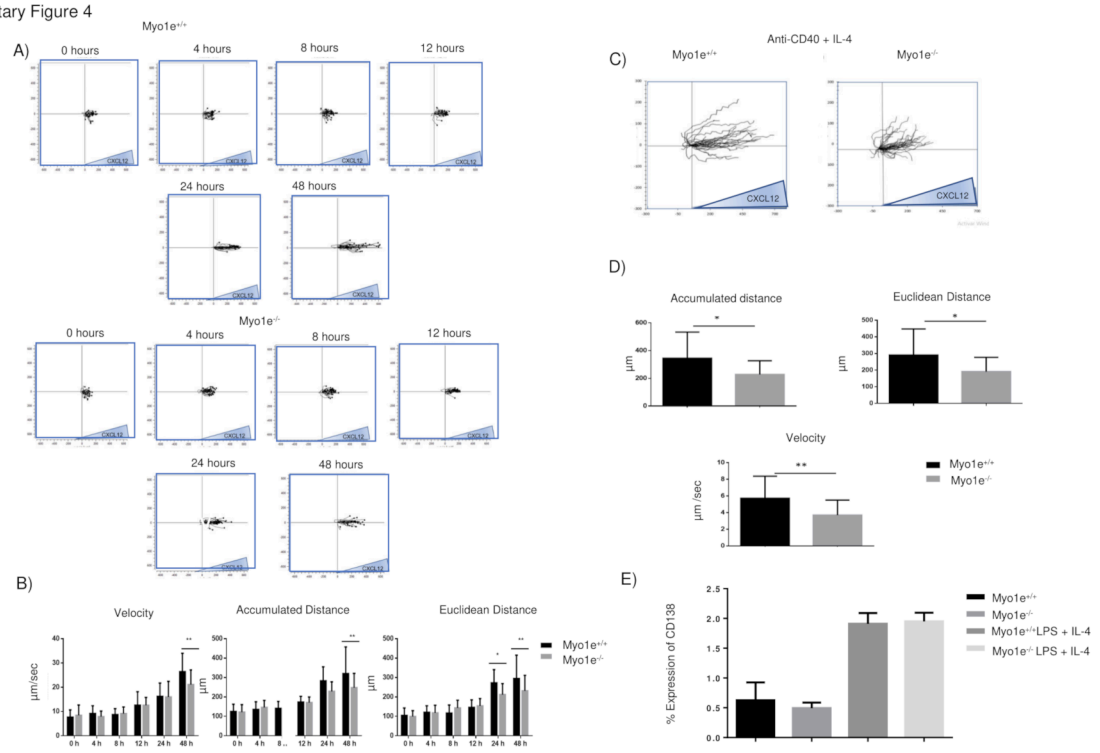

Fig S4. Kinetics of B cell migration in the absence of Myo1e; expression of CD138 by resting and 48 h LPS + IL-4 activated B cells.

A) LPS + IL-4 activated B cells at different times (0, 4, 8, 12, 24, and 48 hours) from of Myo1e$^{+/+}$ and Myo1e$^{-/-}$ mice were deposited in the Zigmond chamber under a CXCL12 gradient, and their migration was registered for 1 hour. Tracks of individual trajectories are presented in the plots. B) Measurements of the velocity, accumulated, and Euclidean distances in LPS + IL-4 activated B cells stimulated with CXCL12. Data are mean ± SD. **p<0.01 *p<0.05. C) Activated (10 µg/ml anti-CD40 and 10 U/ml of IL-4) B cells from of Myo1e$^{+/+}$ and Myo1e$^{-/-}$ mice were deposited in the Zigmond chamber under a CXCL12 gradient and registered for 1 hour. Tracks of individual trajectories are presented in the plots; n=3. D) Measurements of the velocity, accumulated, and Euclidian distances in anti-CD40 + IL-4 activated B cells stimulated with CXCL12; n=3. Data are mean ± SD. **p<0.01 *p<0.05. E) Percentage of the expression of CD138 in resting and activated B cells from Myo1e$^{+/+}$ and Myo1e$^{-/-}$ mice; n=3. Data are mean ± SD.

Supplementary Figure 5

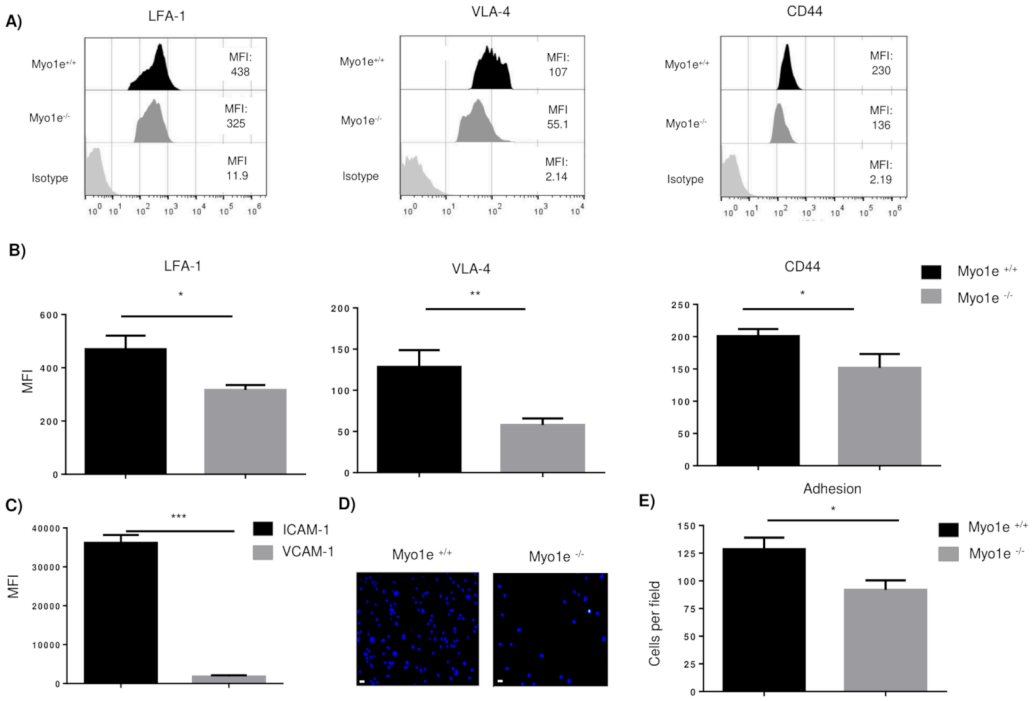

Fig. S5. Myo1e is required for cellular adhesion and allows efficient expression of adhesion molecules

A) Histograms of LFA-1, VLA-4, and CD44 on activated B cells from Myo1e$^{+/+}$ and Myo1e$^{-/-}$ mice; n=5 B) Mean fluorescence intensity of LFA-1, VLA-4, and CD44 in activated B cells from Myo1e$^{+/+}$ and Myo1e$^{-/-}$ mice; n=5. Data are presented as mean ± SD. **p<0.01 *p<0.05. C) Mean fluorescence intensity of ICAM-1 and VCAM-1 on the b-End3 cells; n=3. Data are mean ± SD, *** p<0.001 D) Representative images (10x objective) of activated B cells (stained with Hoechst 33342) from Myo1e$^{+/+}$ and Myo1e$^{-/-}$ mice. The cells were seeded over bEnd.3 cells, after four hours adhesion, unbound cells were washed out, and attached B cells were registered by epifluorescence microscopy. Scale bar 5 μm; n=3. E) Numbers of adherent Myo1e$^{+/+}$ and Myo1e$^{-/-}$ B cells, quantified in 12 fields; n=3. Data are mean ± SD. *p<0.05.

Supplementary Figure 6

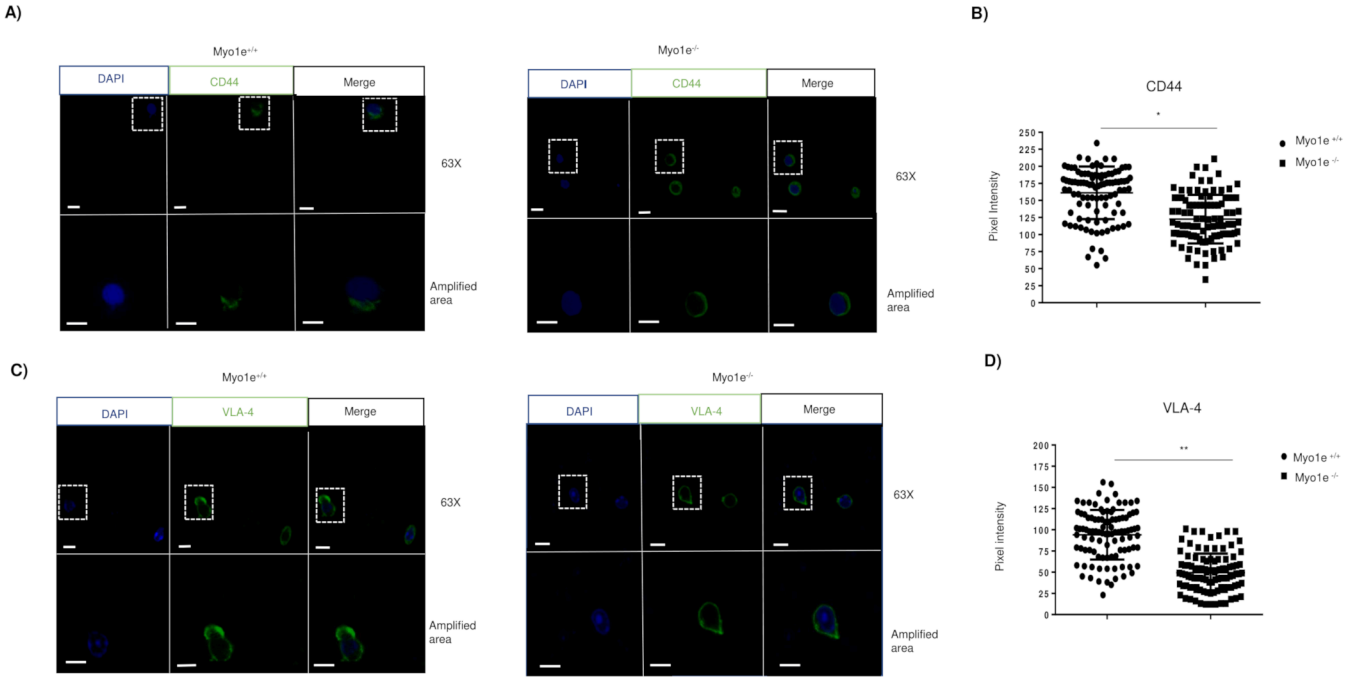

Fig. S6. The absence of Myo1e causes a reduction in the accumulation of CD44 and VLA-4 in the protrusions of membrane

A) Representatives images (63x objective) of activated (LPS + IL-4) B cells from of Myo1e$^{+/+}$ and Myo1e$^{-/-}$ mice, under a CXCL12 gradient. The cells were stained with anti-CD44 and DAPI. Scale bars 5 µm (Amplified area, zoom 2.5) B) The Pixel intensity of CD44 in the protrusion of membrane of activated B cells from of Myo1e$^{+/+}$ and Myo1e$^{-/-}$ mice was measured; n=3. Data are mean ± SD, *p<0.05 C) Representative images (63x objective) of activated (LPS + IL-4) B cells from of Myo1e$^{+/+}$ and Myo1e$^{-/-}$ mice, under a CXCL12 gradient. The cells were stained with anti-VLA-4 and DAPI. Scale bars 5 µm. (Amplified area, zoom 2.5) D) The pixel intensity of VLA-4 in the protrusion of membrane of activated B cells from of Myo1e$^{+/+}$ and Myo1e$^{-/-}$ mice; was measured; n=3. Data are mean ± SD, **p<0.01.

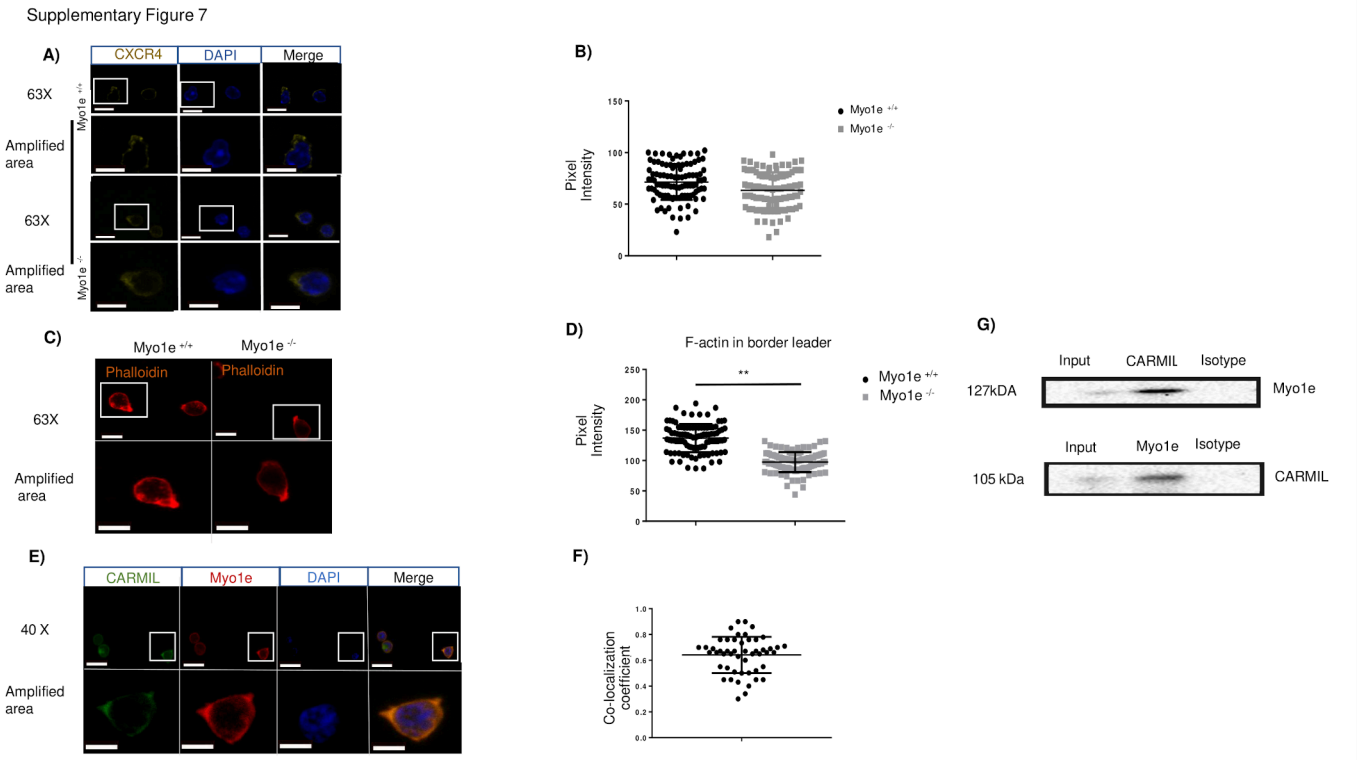

Fig. S7. The lack of Myo1e causes a reduction of F-actin in the border leader of B cells

A) Representative images (63x objective) of CXCR4 in the border-leader of Myo1e$^{+/+}$ and Myo1e$^{-/-}$ B cells stimulated by a gradient of CXCL12. Scale bars 5 μm; (Amplified area, zoom 2.5); n=3. B) Quantification of the pixel intensity of CXCR4 in the protrusion of activated B cells from Myo1e$^{+/+}$ and Myo1e$^{-/-}$ mice. Data were acquired from 50 cells per experiment; n=3. Data are mean ± SD.C) Representatives images (63x objective) of activated B cells from of Myo1e$^{+/+}$ and Myo1e$^{-/-}$ mice under a gradient of CXCL12. The cells were stained with TRITC-phalloidin (Red). Scale bars 5 μm; (Amplified area, zoom 2.5) n=5. D) The pixel intensity of F-actin in the protrusions of the membrane was quantified; n=5. Data are mean ± SD. **p<0.01. E) Representatives images (40x objective) of activated B cells from Myo1e$^{+/+}$ mice stained with anti-Myo1e (Red), anti-CARMIL (Green), and DAPI (Blue). Scale bars 5 μm; (Amplified area, zoom 2.5), n=3. F) Co-localization assays using Pearson's correlation index of Myo1e with CARMIL. The co-localization was measured in 50 cells per experiment; n=3. Data are mean ± SD. G) Co-immunoprecipitation of Myo1e with CARMIL in activated B cells from Myo1e$^{+/+}$ mice, n=3.

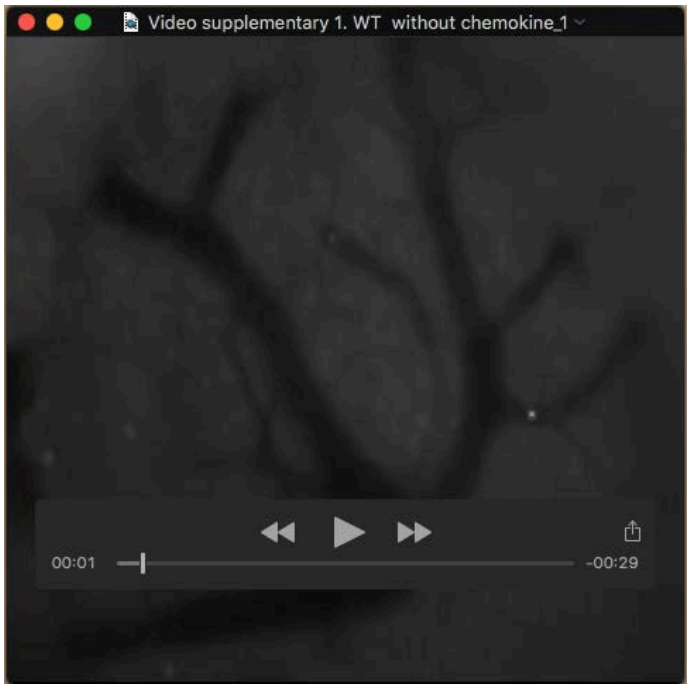

Movie 1

Activated Myo1e$^{+/+}$ B cells running through the venules of an inguinal lymph node previously (1 h) inoculated with PBS. (40x objective).

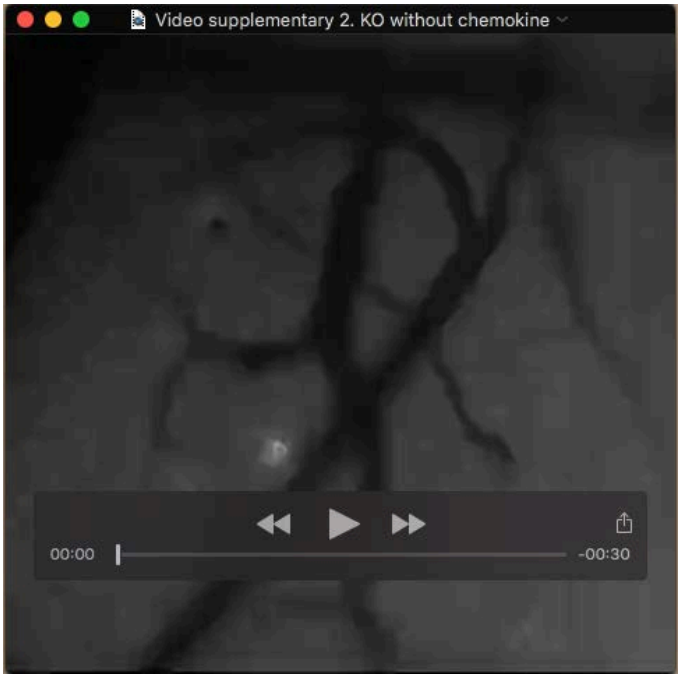

Movie 2

Activated Myo1e$^{-/-}$ B cells running through the venules of an inguinal lymph node previously (1 h) inoculated with PBS. (40x objective).

Journal of Cell Science • Supplementary information

Movie 3

Activated Myo1e$^{+/+}$ B cells running through the venules of an inguinal lymph node previously (1 h) inoculated with CXCL12 (25 ng/ml). (40x objective).

Movie 4

Activated Myo1e$^{-/-}$ B cells running through the venules of an inguinal lymph node previously (1 h) inoculated with CXCL12 (25 ng/ml). (40x objective).

Journal of Cell Science • Supplementary information